Annals of Physics 412 (2020) 168023

Contents lists available at ScienceDirect

Annals of Physics

journal homepage: www.elsevier.com/locate/aop

Tricritical point and solid/liquid/gas phase transition of higher dimensional AdS black hole in massive gravity

Bo Liu [a,b,d], Zhan-Ying Yang [a,c], Rui-Hong Yue [d,*]

[a] School of Physics, Northwest University, Xi'an, 710127, PR China
[b] School of Arts and Sciences, Shaanxi University of Science and Technology, Xi'an, 710021, PR China
[c] Shaanxi Key Laboratory for Theoretical Physics Frontiers, Xi'an 710127, PR China
[d] Center for Gravity and Cosmology, College of physical science and technology, Yangzhou University, Yangzhou, 225009, PR China

ARTICLE INFO

Article history:
Received 13 April 2019
Accepted 3 November 2019
Available online 11 November 2019

Keywords:
Solid/liquid/gas phase transition
Triple critical point
Extended phase space
Massive gravity

ABSTRACT

By considering the fifth order graviton term in massive gravity theory, we study the P–V critical behaviors of AdS black hole in $d \geq 7$ dimensional space–time, and find the solid/liquid/gas phase transition with the "common" tricritical point, which does not exist in absence of higher graviton terms. Moreover, we also find the number of positive real roots of critical radius equation plays a key role in classifying different kinds of phase transitions. If there is only one positive root of equation, the first order Van der Waals-like phase transition emerges. For two roots, the system could experience a zero-order reentrant phase transition. Notably, for three roots, the solid/liquid/gas phase transition can occur. In addition, because the critical radius equation is a $(n-2)$-order polynomial equation associated with the graviton terms, the critical phenomena of black holes in extended phase space depend crucially on the number n of the graviton terms in high dimensional massive gravity.

1. Introduction

Thermodynamics of black hole revealing the relationship between the gravity and thermodynamics has always been one of the hot topics in theoretical physics since the Hawking radiation

* Corresponding author.
E-mail address: rhyue@yzu.edu.cn (R.-H. Yue).

https://doi.org/10.1016/j.aop.2019.168023
0003-4916/

was discovered in 1975 [1]. In recent two decades, more and more attentions are paid on the thermodynamics of black hole in anti-de Sitter (AdS) space. One of the reason is that the AdS black hole can be in thermodynamical stable equilibrium with a positive specific heat, and has Hawking–Page (HP) phase transition between thermal gas and black hole in AdS space [2], which is absent in asymptotically flat or de Sitter space. Another reason is that the AdS/CFT correspondence [3–6], connecting gravity theory in bulk with a conformal field theory on the boundary of AdS space, is regarded as a powerful tool for understanding the strongly correlated system by investigating the classical gravity theory. In this view, HP phase transition could correspond to the confinement/deconfinement phase transition in gauge field theory [7].

In 2012, treating the cosmological constant as the thermodynamical pressure, a first-order phase transition between large and small black hole (LBH/SBH) was discovered [8], whose critical behaviors and exponents are precisely identical with the Van der Waals (VDW) liquid–gas system. In this extended phase space, the black hole mass M should be treated as enthalpy rather than the internal energy [9], and the thermodynamical volume conjugate with the pressure of black hole can be calculated by using the standard thermodynamic identities [10–15]. Then this P–V behavior was generalized into the Born–Infeld AdS black hole [16]. There exists a zero-order reentrant phase transition between intermediate black hole and small black hole along with LBH/SBH phase transition, which is a phase transition from large black holes to small ones and then back to large one again with increasing the temperature, a phenomenon also seen for the singly spinning rotating higher-dimensional rotating AdS black hole [17]. Moreover, in multi-spinning higher-dimensional AdS black hole [18], the system has a small/intermediate/large black hole (S/I/L BH) phase transition with one tricritical (or triple critical) point reminiscent of the "water-like" solid/liquid/gas phase transition. Then, more P–V behaviors for other kinds of AdS black holes were discussed in [19–40].

Among previous studies on these P–V critical behaviors of AdS black holes, to the best of our knowledge, they paid more attention on the existence of different kinds of phase transitions. But it is still unclear for an easy and effective classification of different kinds of phase transitions in extended phase space of AdS black holes, which is still an open and interesting issue. This is one of motivations to our paper.

On the other hand, from the perspective of modern particle physics, the Einstein's general relativity (GR) can be treated as a unique theory of a massless spin-2 graviton [41,42]. Despite many successes agreement with observations, GR might be searched for alternatives due to the open questions, such as the old cosmological constant problem [43] and the origin of acceleration of our universe indicated from the supernova data [44,45], and so on. Massive gravity is a straightforward and natural modification by simply giving a mass to the graviton, which can date back to 1939 when Fierz and Pauli (FP) [46] constructed a linear theory of massive gravity. Then it was generalized in non-linear level to solve the vDVZ discontinuity [47,48], which means that the FP theory could not go back to GR by Einstein in the massless limit. But this non-linear theory still has an elementary problem, so-called the Boulware–Deser ghost [49,50], due to the absence of a Hamiltonian constraint in the Arnowitt–Deser–Misner language [51]. Fortunately,a ghost-free massive theory in four dimension was proposed in [52,53] known as dGRT massive gravity. This theory provides a reference metric where the graviton propagates, and introduces a set of possible interaction terms associated with graviton up to the fourth order. Because it is still ghost-free with an arbitrary reference metric [54], this theory can be extended to bi-gravities [55], a more general scenario with a dynamical reference metric. More details about dGRT massive gravity can be found in review papers [56,57]. Inspired of AdS/CFT correspondence and string theory, the higher dimensional extension of the massive (bi)gravity has been discussed in Ref [58,59], which eliminates ghost fields using the Cayley–Hamilton theorem. And it has also shown that the additional higher dimensional graviton terms, e.g., $U_{i\geq 5}$ should not been neglected. Especially in Ref [60], five-dimensional massive (bi-)gravity has been constructed and a class of physical metrics have been found, such as the Friedmann–Lemaitre–Robertson–Walker, Bianchi type I, and Schwarzschild–Tangherlini metrics, for which the fifth order graviton term U_5 also behaves as an effective cosmological constant. Then in Ref [61], Cayley–Hamilton theorem is shown to be an effective method to construct any $d \geq 4$-dimensional graviton terms and it is proved the existence of the solutions of Schwarzschild–Tangherlini black holes. Hence, studying the dRGT theory and

its extensions with specific higher dimensional graviton terms in higher dimensions is physically important.

Interestingly, a class of charged black holes were found in [62] and their corresponding thermodynamics [63] in AdS space–time were investigated in massive gravity. It is shown that the coefficients for the third and/or fourth potential term in higher dimension play the key role in the phase space. The other black hole solutions and their thermodynamic properties have been investigated in dGRT massive gravity [64–67]. Particularly in the extended phase space, the VDW-like phase transition was found in the charged AdS black hole in massive gravity [68], which was also found in Refs [69–74]. In the higher dimensional ($d \geq 6$) space–time, the reentrant phase transitions [75] could appear in this P–V process in massive gravity. Moreover, investigating in the extensions of massive gravity, more interesting and richer P–V critical phenomena were found [76], including the solid/liquid/gas phase transitions. Recently, the holographic and thermodynamic aspects of black holes in massive gravity are also investigated in Refs [77,78]. In addition, the references [79,80] show that massive gravity parameters modify the efficiency of heat engine on a significant level.

Up to now, there are still few studies on the aspects of black holes in higher dimensional (bi-) massive gravity with higher order graviton terms. Most of researches in higher dimensional space–time focus only on five or/and six dimensions [69–76], where the higher order graviton terms $\mathcal{U}_{i\geq 5}$ vanish due to the constraint condition [57], which indicates that the terms of $\mathcal{U}_{d-1}$ and $\mathcal{U}_d$ associated with reference metric will vanish in d-dimensional space–time. This may be one reason why the higher order graviton terms are paid less attention. To the best of our knowledge, there has been a paper [81] discussing the critical behavior and phase transitions of AdS black hole solutions in the Lovelock massive gravity with higher order graviton terms. However, the fifth graviton term is considered as the high order small quantity which is ignored in the following calculations.

Taking these considerations seriously, in this paper we will concentrate on the critical behaviors of $d \geq 7$-dimensional AdS black hole in dRGT theory with higher-order graviton terms. The organization of this paper is as follows. In Section 2, considering only the fifth order graviton term of massive gravity in $d \geq 7$ dimensional space–time, we present the thermodynamics in extended phase space of higher-dimensional AdS black hole. In Section 3, we study the behaviors of $d \geq 7$ dimensional AdS black hole, and reveal the richer critical phenomena in the context of P–V criticality and phase diagrams. Finally, a brief discussion is presented in Section 4.

2. Extended phase space thermodynamics of higher-dimensional AdS black hole in massive gravity

Let us start with the action for d-dimensional massive gravity in the geometric units $G_N = \hbar = c = k = 1$ [56,57]

$$I = \frac{1}{16\pi}\int d^dx\sqrt{-g}\Big[R + \Lambda + m^2\sum_{i=1}^{n} c_i\mathcal{U}_i(g,f)\Big], \tag{1}$$

where the last term denotes general form of the interaction potential with graviton mass m, and $n \leq d-2$ the number of dimensionless coupling coefficients c_i. Moreover, f is a fixed rank-2 symmetric tensor, and $\mathcal{U}_i$ are symmetric polynomials of the eigenvalues of the $d \times d$ matrix $K^\mu_\nu = \sqrt{g^{\mu\alpha}f_{\alpha\nu}}$, and satisfying the following recursion relation

$$\mathcal{U}_i = -\sum_{j=1}^{i}(-1)^j\frac{(i-1)!}{(i-j)!}[K^j]\mathcal{U}_{i-j}. \tag{2}$$

Obviously, the first few terms can be read as

$$\begin{aligned}\mathcal{U}_1 &= [K],\\ \mathcal{U}_2 &= [K]^2 - [K^2],\\ \mathcal{U}_3 &= [K]^3 - 3[K][K^2] + 2[K^3],\end{aligned} \tag{3}$$

$$\begin{aligned}
\mathcal{U}_4 &= [K]^4 - 6[K^2][K]^2 + 8[K^3][K] + 3[K^2]^2 - 6[K^4],\\
\mathcal{U}_5 &= [K]^5 - 10[K^2][K]^3 + 15[K][K^2]^2 + 20[K]^2[K^3] - 20[K^2][K^3] - 30[K][K^4] + 24[K^5],\\
&\cdots
\end{aligned}$$

where the square brackets denote traces, i.e. $[K] = K^{\mu}_{\mu}$.

A static black hole solution of d-dimensional space–time is given as

$$ds^2 = -f(r)dt^2 + f^{-1}(r)dr^2 + r^2 h_{ij}dx^i dx^j, \tag{4}$$

in which $h_{ij}dx^i dx^j$ is the line element for an Einstein space with constant curvature $(d-2)(d-3)k$, and $k = 1, 0, -1$ correspond respectively to a spherical, Ricci flat, and hyperbolic topology subspace. Considering the following reference metric

$$f_{\mu\nu} = diag(0, 0, c_0^2 h_{ij}), \tag{5}$$

the interaction potential Eq. (3) changes into

$$\mathcal{U}_j = \Big(\prod_{k=2}^{j+1} d_k\Big) c_0^j r^{-j} \tag{6}$$

with positive constant c_0 and the notation $d_k = (d-k)$. It is worth to note that the $c_5 m^2$ term only appears in the action for $d \geq 7$, so we just consider the $d \geq 7$ dimensional black hole and $n = 5$ in this paper.

Then, the metric function is calculated as

$$\begin{aligned}
f(r) =& k + \frac{16\pi P}{d_1 d_2} r^2 - \frac{16\pi M}{d_2 V_{d-2} r^{d-3}} + \frac{c_0 c_1 m^2}{d_2} r + c_0^2 c_2 m^2\\
&+ \frac{d_3 c_0^3 c_3 m^2}{r} + \frac{d_3 d_4 c_0^4 c_4 m^2}{r^2} + \frac{d_3 d_4 d_5 c_0^5 c_5 m^2}{r^3},
\end{aligned} \tag{7}$$

here V_{d-2} is the volume of subspace spanned by coordinates x^i, M is the mass of black hole, and $P = \frac{d_1 d_2}{16\pi l^2}$ is the pressure.

According to the relation $f(r_h) = 0$ which determines the horizon of black hole, the mass of black hole can be expressed in terms of r_h as

$$\begin{aligned}
M =& \frac{d_2 V_{d-2} r_h^{d-3}}{16\pi}\Big[k + \frac{16\pi P}{d_1 d_2} r_h^2 + \frac{c_0 c_1 m^2}{d_2} r_h + c_0^2 c_2 m^2 + \frac{d_3 c_0^3 c_3 m^2}{r_h}\\
&+ \frac{d_3 d_4 c_0^4 c_4 m^2}{r_h^2} + \frac{d_3 d_4 d_5 c_0^5 c_5 m^2}{r_h^3}\Big].
\end{aligned} \tag{8}$$

And the Hawking temperature T and the entropy S of black hole can be obtained as

$$\begin{aligned}
T =& \frac{1}{4\pi r_h}\Big[d_3 k + \frac{16\pi P}{d_2} r_h^2 + c_0 c_1 m^2 r_h + d_3 c_0^2 c_2 m^2 + \frac{d_3 d_4 c_0^3 c_3 m^2}{r_h}\\
&+ \frac{d_3 d_4 d_5 c_0^4 c_4 m^2}{r_h^2} + \frac{d_3 d_4 d_5 d_6 c_0^5 c_5 m^2}{r_h^3}\Big]\\
S =& \frac{V_{d-2}}{4} r_h^{d-2}.
\end{aligned} \tag{9}$$

Due to the mass of black hole corresponding to the enthalpy of an AdS gravitational system, we can get the Smarr relation as follows using the scaling method

$$\begin{aligned}
(d-3)M =& (d-2)TS - 2PV - \frac{c_0 c_1 m^2 V_{d-2} r_h^{d-2}}{16\pi} + \frac{d_2 d_3 c_0^3 c_3 m^2 V_{d-2} r_h^{d-4}}{16\pi}\\
&+ \frac{d_2 d_3 d_4 c_0^4 c_4 m^2 V_{d-2} r_h^{d-5}}{8\pi} + \frac{3 d_2 d_3 d_4 d_5 c_0^5 c_5 m^2 V_{d-2} r_h^{d-6}}{16\pi},
\end{aligned} \tag{10}$$

where $V = \frac{V_{d-2}}{d-1} r_h^{d-1}$ denotes the thermodynamic volume conjugate with the pressure $P = -\frac{\Lambda}{8\pi} = \frac{(d-1)(d-2)}{16\pi l^2}$, and l is the radius of d-dimensional AdS space–time. Moreover, the first law of black hole thermodynamics can be written as the following differential relation

$$\begin{aligned} dM =& TdS + VdP + \frac{c_0 m^2 V_{d-2} r_h^{d-2}}{16\pi} dc_1 + \frac{d_2 c_0^2 m^2 V_{d-2} r_h^{d-3}}{16\pi} dc_2 + \frac{d_2 d_3 c_0^3 m^2 V_{d-2} r_h^{d-4}}{16\pi} dc_3 \\ &+ \frac{d_2 d_3 d_4 c_0^4 m^2 V_{d-2} r_h^{d-5}}{16\pi} dc_4 + \frac{d_2 d_3 d_4 d_5 c_0^5 m^2 V_{d-2} r_h^{d-6}}{16\pi} dc_5. \end{aligned} \tag{11}$$

Obeying the thermodynamical formulas, the Gibbs free energy can be written as

$$\begin{aligned} G &= M - TS \\ &= -\frac{V_{d-2} r_h^{d-3}}{2} \left[\frac{2P r_h^2}{d_1 d_2} - \frac{k + c_0^2 c_2 m^2}{8\pi} - \frac{d_3 c_0^3 c_3 m^2}{4\pi r_h} - \frac{3 d_3 d_4 c_0^4 c_4 m^2}{8\pi r_h^2} - \frac{d_3 d_4 d_5 c_0^5 c_5 m^2}{2\pi r_h^3} \right]. \end{aligned} \tag{12}$$

3. Critical behaviors of higher-dimensional black hole

3.1. Equation of state

With the help of Eq. (9), the equation of state of black hole $P(V, T)$ can be written as

$$\begin{aligned} P =& \frac{d_2}{4 r_h} \left[T - \frac{d_3 k}{4\pi r_h} - \frac{c_0 c_1 m^2}{4\pi} - \frac{d_3 c_0^2 c_2 m^2}{4\pi r_h} - \frac{d_3 d_4 c_0^3 c_3 m^2}{4\pi r_h^2} \right. \\ &\left. - \frac{d_3 d_4 d_5 c_0^4 c_4 m^2}{4\pi r_h^3} - \frac{d_3 d_4 d_5 d_6 c_0^5 c_5 m^2}{4\pi r_h^4} \right]. \end{aligned} \tag{13}$$

Comparing Eq. (13) to the equation of state of the Van der Waals fluid, we can identify the special volume of the black hole as

$$v = \frac{4 r_h}{d-2} \propto r_h \tag{14}$$

For the further convenience, we introduce the following denotations

$$\begin{aligned} &\hat{T} = T - \frac{c_0 c_1 m^2}{4\pi}; \quad \omega_2 = -\frac{k + c_0^2 c_2 m^2}{8\pi}; \\ &\omega_3 = -\frac{c_0^3 c_3 m^2}{8\pi}; \quad \omega_4 = -\frac{c_0^4 c_4 m^2}{8\pi}; \quad \omega_5 = -\frac{c_0^5 c_5 m^2}{8\pi} \end{aligned} \tag{15}$$

where $\hat{T}$ is called shifted temperature and could be negative value.

Using the condition of inflection point in Van der Walls system

$$\left. \frac{\partial P}{\partial r_h} \right|_{\hat{T}=\hat{T}_c, r_h=r_c} = \left. \frac{\partial^2 P}{\partial r_h^2} \right|_{\hat{T}=\hat{T}_c, r_h=r_c} = 0, \tag{16}$$

we can receive the critical shifted temperature and the equation of critical radius of black hole as

$$\hat{T}_c = -\frac{2 d_3}{r_c} \left[2\omega_2 + \frac{3 d_4 \omega_3}{r_c} + \frac{4 d_4 d_5 \omega_4}{r_c^2} + \frac{5 d_4 d_5 d_6 \omega_5}{r_c^3} \right] \tag{17}$$

$$\omega_2 r_c^3 + 3 d_4 \omega_3 r_c^2 + 6 d_4 d_5 \omega_4 r_c + 10 d_4 d_5 d_6 \omega_5 = 0 \tag{18}$$

In the case of $\omega_2 = 0$, or $\omega_5 = 0$, one can easily find that Eq. (18) has at most two positive real roots corresponding to the critical radii of black hole, the critical behaviors are similar to the ones in reference [75]. We neglected it and focus only on the case of $\omega_2 \neq 0$, $\omega_5 \neq 0$, where exists probably three critical radii.

For the simplicity, denoting

$$\alpha = 3 d_4 \omega_3 / \omega_2, \quad \beta = 6 d_4 d_5 \omega_4 / \omega_2, \quad \gamma = 10 d_4 d_5 d_6 \omega_5 / \omega_2, \tag{19}$$

Table 1
The behaviors of the critical radii for different values of β and γ with $\gamma_{\pm} = \frac{2-9\beta\pm 2(1-3\beta)^{3/2}}{27}$.

Parameters	$\alpha = -1$				
β	$1/4 < \beta < 1/3$	$0 < \beta \leq 1/4$		$\beta \leq 0$	
γ	$\gamma_- < \gamma < \gamma_+$	$\gamma_- < \gamma < 0$	$0 < \gamma < \gamma_+$	$0 < \gamma < \gamma_+$	$\gamma_- < \gamma < 0$
Number of r_c	3	3	2	2	1

the critical temperature and pressure become

$$\hat{T}_c = -\frac{2d_3\omega_2}{r_c}\left[2 + \frac{\alpha}{r_c} + \frac{2\beta}{3r_c^2} + \frac{\gamma}{2r_c^3}\right]$$
$$\hat{P}_c = -\frac{2d_2d_3\omega_2}{r_c^2}\left[2 + \frac{5\alpha}{3r_c} + \frac{\beta}{r_c^2} + \frac{4\gamma}{5r_c^3}\right], \tag{20}$$

which just depends on the dimension of space–time by a factor d_2d_3 (d_3) for given parameters (ω_2, α, β, γ).

It is easy to find that Eq. (18) has at most two positive roots in the case $\alpha \geq 0$, whereas there would exist three real roots if $\alpha < 0$. Since the value of α could be set to be one by re-scaling r_c, we will assume $\alpha = -1$ in following discussion. Based on the requirement of three real roots of Eq. (18), we can obtain the relation between the parameters and the number of positive real roots in Table 1.

Due to the positive pressures, when all of the pressures $P_{c1,2,3}$ corresponding to the critical radii above are positive, we can obtain three critical points in the P–V process, and when two of $P_{c1,2,3}$ are positive, we will get two critical points, and so on. For example, taking $d = 7$ and letting $\omega_2 = \pm 1$ we will get three positive corresponding pressures while $\omega_2 = -1,\ 2/9 < \beta < 1/4,\ \gamma_p < \gamma < 0$, or $\omega_2 = -1,\ 1/4 < \beta < 1/3,\ \gamma_p < \gamma < 0$, where γ_p must be determined numerically.

According to the Gibbs free energy Eq. (12) and the equation of state Eq. (13), let us now study the possible phase transitions of this system.

3.2. Van der Waals-like phase transition

In the case of one critical radius of Eq. (18) in Table 1, the critical behaviors of black hole are analogous to that of the standard Van der Waals-like system as displayed in Fig. 1.

In Fig. 1(a), there is only one critical isotherm (red dashed line) when $\hat{T} = \hat{T}_c \approx 5.51733$, and exits an inflection point in the isotherm (the green solid line) when $\hat{T} < \hat{T}_c$. Moreover, Fig. 1(b) depicts the behaviors of G with a critical isobar (red dashed line) when $P = P_c \approx 1.48178$, the isobar corresponding to $P < P_c$ is depicted with a "swallowtail", which implies a first-order LBH/SBH phase transition.

3.3. Reentrant phase transition

There are two ranges of parameters for two critical radii in Table 1, both of which display the similar thermodynamical processes with a reentrant phase transition, analogous to that in references [16,17,75]. In one case, by setting $\beta = 0.245$ and $\gamma = 0.0001$, the critical behaviors are investigated as follows.

In the P–r_h processes indicated in Fig. 2(a), there exist two critical isotherms, $\hat{T} = \hat{T}_{c1} \approx 10.50671$ and $\hat{T} = \hat{T}_{c2} \approx 10.38895$, corresponding respectively to the red and black dashed lines. Moreover, there are two inflection points located in each isotherm of the branch corresponding to $\hat{T}_{c2} < \hat{T} < \hat{T}_{c1}$ as displayed by the blue solid isotherm.

The behaviors of Gibbs free energy G are displayed in Fig. 2(b), where the radius of black hole increases from right to left along each isobar, and two critical isobars, the red and black dashed lines, correspond respectively to the critical pressures $P = P_{c1} \approx 6.39165$ and $P = P_{c2} \approx 6.09163$. The magenta solid isobar corresponds to the tricritical point, ($\hat{T}_{tr} \approx 10.44195$, $P_{tr} \approx 6.25396$), while

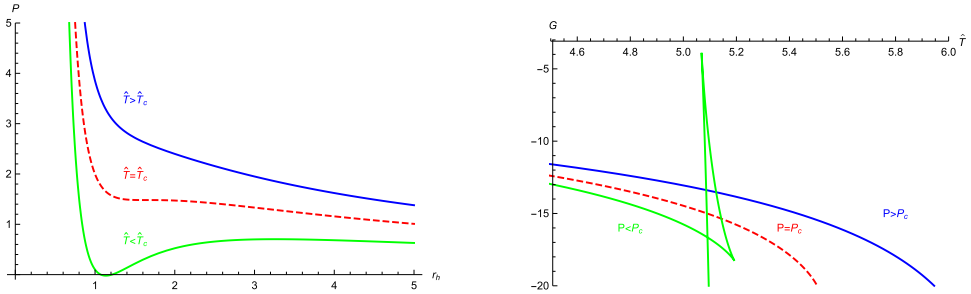

(a)$P-r_h$ (b)$G-\hat{T}$

Fig. 1. The P–r_h and G–T diagrams in $d=7$ with $\omega_2=-1$, $\alpha=-1$, $\beta=-1$, $\gamma=-0.1$.

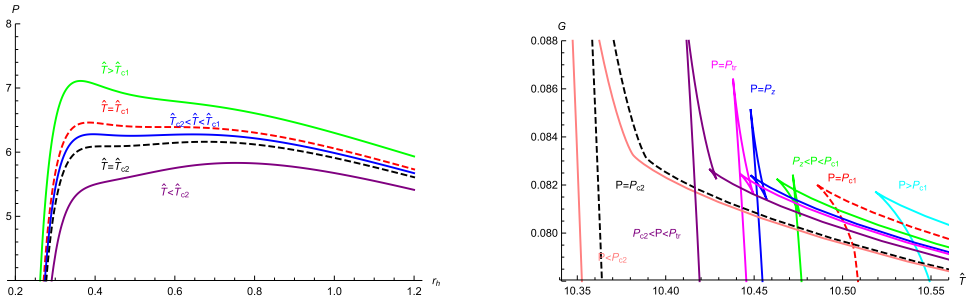

(a)$P-r_h$ diagram (b)$G-\hat{T}$ diagram

Fig. 2. The P–r_h and G–$\hat{T}$ diagrams in $d=7$ with $\omega_2=-1$, $\alpha=-1$, $\beta=0.245$, $\gamma=0.0001$.

the blue one to ($\hat{T}_z\approx 10.44797$, $P_z\approx 6.27301$). As the temperature decreases from right to left, in the range $P\in(P_z,P_{c1})$ and $\hat{T}\in(\hat{T}_z,\hat{T}_{c1})$, there is a "swallowtail" indicated by the green solid isobar signifying a Van der Waals-like phase transition. In the range $P\in(P_{c2},P_{tr})$ and $\hat{T}\in(\hat{T}_{c2},\hat{T}_{tr})$, a "swallowtail" displayed by the purple isobar, does not correspond to the Van der Waals-like phase transition, because it is not a "physical" process due to the global minimum of the Gibbs free energy as shown in Fig. 3(a), so that ($\hat{T}_{c2}$, P_{c2}) is not a "really and physically" critical point.

Especially in the ranges $P\in(P_{tr},P_z)$ and $\hat{T}\in(\hat{T}_{tr},\hat{T}_z)$, the global minimum of G is discontinuous as the temperature increases. As displayed in Fig. 3(b), the value of G experiences a finite jump at $\hat{T}=\hat{T}_0\approx 10.44382\in(\hat{T}_{tr},\hat{T}_z)$ due to the global minimum of the Gibbs free energy, which signifies the zero-order reentrant phase transition between small and intermediate black holes.

It is obviously found in P–$\hat{T}$ phase diagram in Fig. 4(a), that the red line in the inset, initiating from the triple critical point ($\hat{T}_{tr}$, P_{tr}) and terminating at ($\hat{T}_z$, P_z), corresponds to the coexistence line between IBH and SBH, while the blue one, initiating from ($\hat{T}_{tr}$, P_{tr}) and terminating at ($\hat{T}_{c1}$, P_{c1}), to the coexistence line of SBH and LBH. It is worth to state that, in the range $P<P_{tr}$ and $\hat{T}<\hat{T}_{tr}$, there is no phase transition between SBH (or IBH) and LBH so that the ($\hat{T}_{tr}$, P_{tr}) is unlike the common one of water.

In another case, by setting $\beta=-1$ and $\gamma=0.85$, the critical behaviors are analogous to those in preceding case ($\beta=0.245$ and $\gamma=0.0001$), since the P–$\hat{T}$ phase diagram in Fig. 4(b) is obviously similar to the one in Fig. 4(a). In Fig. 4(b), the "physical" critical point is ($\hat{T}_{c1}\approx 6.34216$, $P_{c1}\approx 2.05297$), the tricritical point is ($\hat{T}_{tr}\approx 5.75374$, $P_{tr}\approx 1.57488$), and the termination point of reentrant phase transition is ($\hat{T}_z\approx 5.76867$, $P_z\approx 1.60544$). The blue line corresponds to the

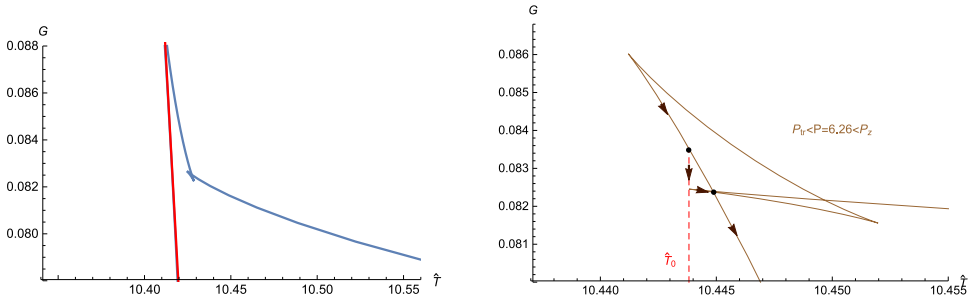

(a)$G-\hat{T}$ diagram (b)Reentrant phase transition

Fig. 3. Diagrams with $d=7$, $\omega_2=-1$, $\alpha=-1$, $\beta=0.245$, $\gamma=0.0001$. (a) For a fixing temperature, a stable "physical" system should be in the state with the global minimum of Gibbs free energy. So, the red line stands for the real and stable state of black hole corresponding to each temperature. (b) Black arrows indicate the real process of the system with temperature increasing due to the global minimum of Gibbs free energy.

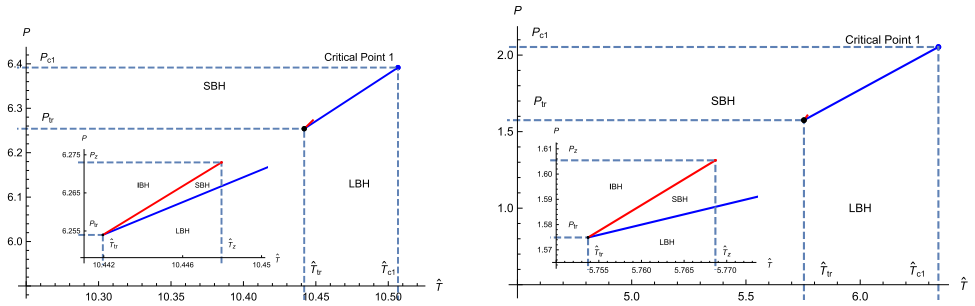

(a)$\beta=0.245$, $\gamma=0.0001$. (b)$\beta=-1$, $\gamma=0.85$

Fig. 4. P–$\hat{T}$ diagrams with $d=7$, $\omega_2=-1$ and $\alpha=-1$.

coexistence line between SBH and LBH, while the red one in the inset to the one between SBH and IBH.

3.4. Triple critical point and solid/liquid/gas phase transition

In the case of three critical radii in Table 1, there are also two cases for different parameters, both of which display the analogous thermodynamical processes as a solid/liquid/gas phase transition with a tricritical (triple critical) point. Therefore, we just focus on one of them by setting $\beta=0.3$, $\gamma=-0.027$.

In Fig. 5(a), the temperature of isotherm increases from lower left to upper right in the P–r_h diagram. Obviously, the P–r_h diagram, which is more complex than that of the standard Van der Waals system, has three critical isotherms, $\hat{T}_{c1}\approx 13.65904$, $\hat{T}_{c2}\approx 11.08718$, $\hat{T}_{c3}\approx 10.37037$, corresponding respectively to purple, black, cyan dashed lines. Particularly, there are three inflection points of each isotherm of the branch in the range $(\hat{T}_{c3}<\hat{T}<\hat{T}_{c2})$, as indicated by the blue one, which may suggest the existence of the more complex phase structures.

The behaviors of Gibbs free energy G of black hole are depicted in Fig. 5(b), where the three critical isobars, $P_{c1}\approx 24.39363$, $P_{c2}\approx 7.24789$, $P_{c3}\approx 4.938276$, are labeled by the purple, black, and cyan dashed lines respectively. The pressure of isobar increases from left to right, and

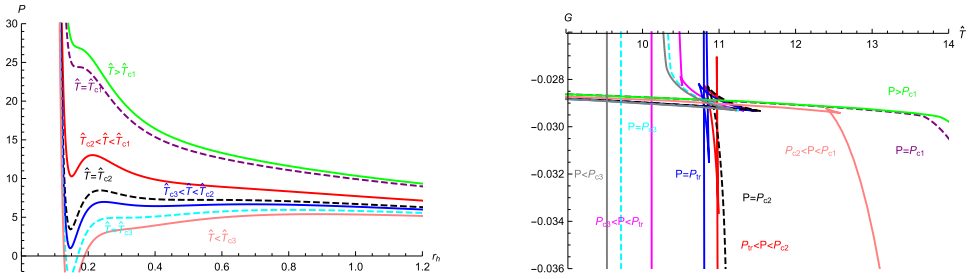

(a)$P - r_h$ diagram (b)$G - \hat{T}$

Fig. 5. P–r_h and G–$\hat{T}$ diagrams with $d = 7$, $\omega_2 = -1$, $\alpha = -1$, $\beta = 0.3$, $\gamma = -0.027$.

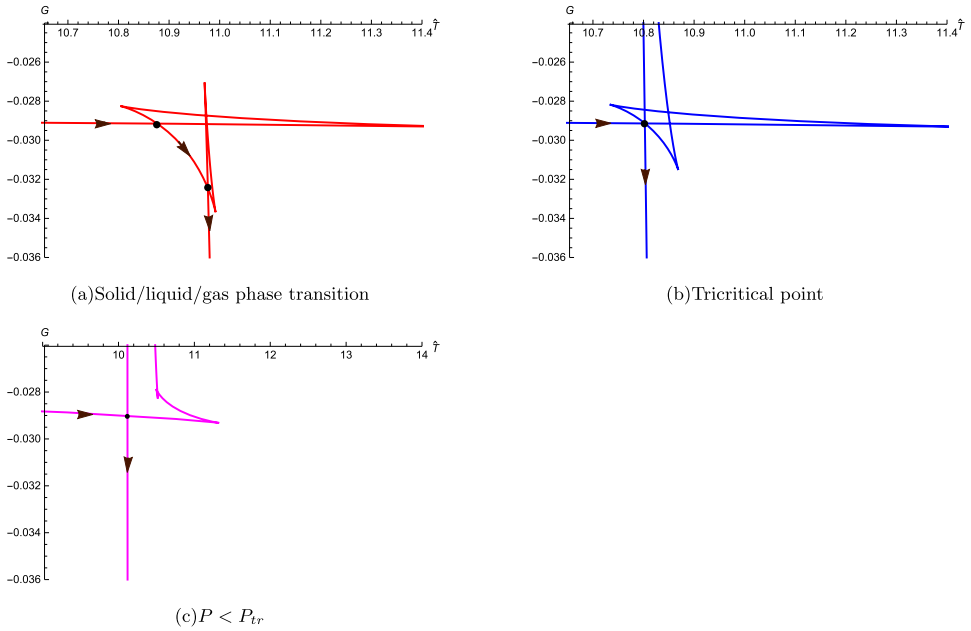

(a)Solid/liquid/gas phase transition (b)Tricritical point

(c)$P < P_{tr}$

Fig. 6. Physical process in G–$\hat{T}$ diagrams. The black arrows show the real and physical process of the system both in (a), (b) and (c), due to the global minimum of Gibbs free energy.

the black hole radius r_h also increases along each isobar from left to right. As the temperature decreases from right to left, for $P > P_{c1}$, there is no critical behavior as shown by the green isobar. For $P_{c2} < P < P_{c1}$ and $\hat{T}_{c2} < \hat{T} < \hat{T}_{c1}$, the pink isobar has one swallowtail, implying a first-order Van der Waals-like phase transition. For $P_{tr} < P < P_{c2}$ and $\hat{T}_{tr} < \hat{T} < \hat{T}_{c2}$, the behaviors are displayed by the red isobar in Fig. 6(a), which shows two swallowtails, corresponding to the coexistence of two first-order phase transitions—SBH/IBH and IBH/LBH phase transitions. Until at $P = P_{tr} \approx 6.64714$ and $\hat{T} = \hat{T}_{tr} \approx 10.80263$ in blue isobar in Fig. 6(b), the two swallowtails merge with each other, corresponding to the tricritical point of the small, intermediate and large black holes. As the temperature continuously decreases, for $P_{c3} < P < P_{tr}$ and $\hat{T}_{c3} < \hat{T} < \hat{T}_{tr}$, the magenta isobar describing the behaviors is also with two swallowtails, but the "small" swallowtail on the upper-right side is not a "really and physical" critical process because of the global minimization of the Gibbs free energy G in Fig. 6(c), similar to the situation of the reentrant phase transition in

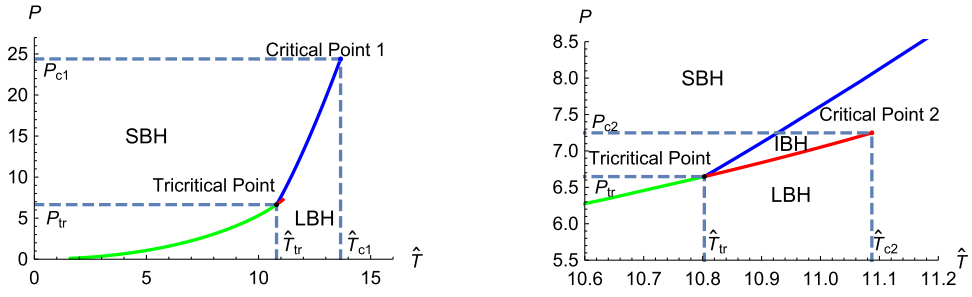

(a)$P-\hat{T}$ diagram (b)Magnification of $P-\hat{T}$ diagram

Fig. 7. The P–$\hat{T}$ diagrams in $d=7$ with $\omega_2=-1$, $\alpha=-1$, $\beta=0.3$, $\gamma=-0.027$.

SubSection 3.3. So only the "big" one left corresponds to the first-order phase transition. Finally, there is also only one swallowtail occurring in the case $P<P_{tr}$, so that the critical point $(P_{c3}, \hat{T}_{c3})$ is not a physically critical one. Therefore, there exist two physically critical points $(P_{c1}, \hat{T}_{c1})$ and $(P_{c2}, \hat{T}_{c2})$ and one tricritical point $(P_{tr}, \hat{T}_{tr})$.

This tricritical behavior of S/I/L BH phase transition is obviously depicted by P–$\hat{T}$ phase diagrams in Fig. 7. These diagrams are analogous to that of the water-like solid/liquid/gas phase transition with a triple critical point. The SBH/LBH coexistence line, denoted in green color and terminating at the tricritical point $(\hat{T}_{tr}, P_{tr})$, corresponds to the solid/gas coexistence line of water. The LBH/IBH and IBH/SBH coexistence lines, depicted respectively by the red and blue ones, do not extend to infinity and terminate respectively at the critical points 1 $(\hat{T}_{c1}, P_{c1})$ and 2 $(\hat{T}_{c2}, P_{c2})$, corresponding respectively to the solid/liquid and liquid/gas coexistence ones of water. Moreover, the join point (or the tricritical point) of the three coexistence lines corresponds to the state of coexistence of small/intermediate/large black holes with a special critical value of temperature and pressure. It is necessary to note that this triple critical point is a more "common" one than that in reentrant phase transition, because there still exists a coexistence line between SBH and LBH when $0<\hat{T}<\hat{T}_{tr}$ and $0<P_{c1}<P_{tr}$, which is not seen in the reentrant phase transition in Figs. 4(a) and 4(b).

By setting $\beta=0.245$, $\gamma=-0.009$ in another case of three critical radii, the "P–V" processes and critical behaviors of G of BH indicated in Fig. 8 are respectively similar to those in Figs. 5 and 6. In Fig. 8(a), the black, magenta, and purple dashed isotherms correspond respectively to the critical temperatures $\hat{T}_{c1}\approx 1967.34429$, $\hat{T}_{c2}\approx 10.23876$, and $\hat{T}_{c3}\approx 8.31659$. Because $\hat{T}_{c1}\gg\hat{T}_{c2},\hat{T}_{c3}$, the pressures of the solid pink, dashed black, and solid green lines are reduced by 2500 times, while the radii enlarged by 9 times, so that all the isotherms can be displayed in one diagram. In Fig. 8(b), the magenta and purple dashed isobars correspond respectively to $P_{c2}\approx 5.94913$, $P_{c3}\approx 0.29619$. The blue isobar has two swallowtails (big one displayed partially in Fig. 8(b)), which implies existence of SBH/IBH and IBH/LBH phase transitions. The red isobar denotes the tricritical point ($T_{tr}\approx 10.07367$, $P_{tr}\approx 5.64492$). Due to $P_{c1}\approx 35484.97609\gg P_{c2},P_{c3}$, the isobars for $P\geq P_{c1}$ are not displayed in this diagram. It is more obvious that the magnification of P–$\hat{T}$ phase diagram near tricritical point in Fig. 9(b) is analogous to the one in Fig. 7(b).

4. Discussion

In this paper, introducing the fifth order graviton term $c_5\mathcal{U}_5$ of interaction potential in massive gravity, we have shown that the solid/liquid/gas phase transition with a "common" tricritical point could appear in the P–V process in the extended phase space of the higher-dimensional AdS black holes. At first, we obtained a class of solutions of AdS black holes in massive gravity theory with fifth term $c_5\mathcal{U}_5$ of interaction potential in the higher dimensional ($d\geq 7$) space–time. Also treating the cosmological constant as pressure and interpreting the corresponding conjugate quantity as thermodynamic volume, we constructed the thermodynamics of black hole in the extend phase

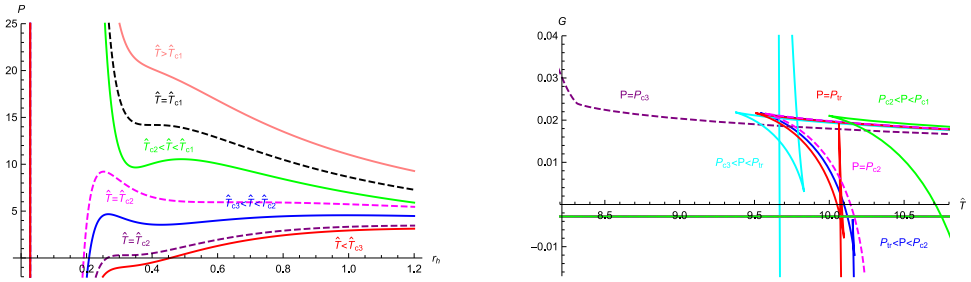

(a)$P-r_h$ (b)$G-\hat{T}$

Fig. 8. The P–r_h and G–$\hat{T}$ diagrams in $d=7$ with $\omega_2=-1$, $\alpha=-1$, $\beta=0.245$, $\gamma=-0.009$.

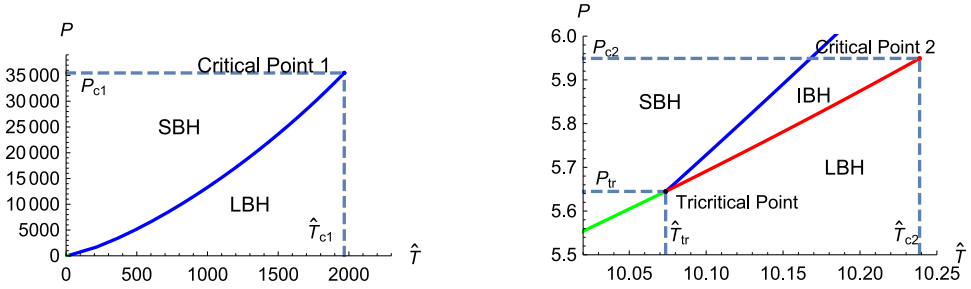

(a)$P-\hat{T}$ diagram (b)Magnification of $P-\hat{T}$ diagram

Fig. 9. The P–$\hat{T}$ diagrams in $d=7$ with $\omega_2=-1$, $\alpha=-1$, $\beta=0.245$, $\gamma=-0.009$.

space. Then, according to the conditions of the inflection point, we got the equations of critical temperature and radius basing on the state equation of this system. Meanwhile, we paid more attention on the case of three real roots of the equation of the critical radius because of the more complex phase construction, and obtained the conditions of parameters corresponding to the number of positive roots or critical radii. Finally, we studied the critical behaviors of the Gibbs free energy of black hole, and found that in the case of three critical radii, there is a SBH/IBH/LBH phase transition similar to water-like solid/liquid/gas one with a "common" triple critical point, where three phase of black hole can coexist with the same values of temperature, pressure and the Gibbs free energy.

Moreover, we find that the number of critical radii of Eq. (18) plays a key role in classification of different kinds of phase transition of AdS black holes in massive gravity. If there is at most one critical radius, it has only first order Van der Waals-like phase transition. For two real critical radii, the system will experience a zero-order reentrant phase transition. Especially for three critical radii, the solid/liquid/gas phase transition can occur with a common triple critical point. In fact, due to more graviton terms appearing in the action in high dimensional massive gravity, the critical radius equation becomes a $(n-2)$-order polynomial equation by choosing the special reference metric. Therefore, the number of roots depends crudely on the number of the graviton terms appearing in the action of the massive gravity. If introducing the higher order graviton terms $c_i\mathcal{U}_i$ $(i \geq 6)$ in high dimensional massive gravity, the black hole will have richer and more fruitful thermodynamical structures and critical behaviors, which are valued to be investigated in future. In addition, the higher order graviton terms should not be ignored, and are important to the studies in high dimensional massive gravity.

Acknowledgments

We would like to thank Dr. Decheng Zou and Dr. Ming Zhang for many discussions. This work was supported by the National Natural Science Foundation of China under Grant No. 11675139, No. 11435006 and No. 11875220.

References

[1] S.W. Hawking, Commun. Math. Phys. 43 (1975) 199.
[2] S. Hawking, D.N. Page, Comm. Math. Phys. 87 (1983) 577.
[3] S.S. Gubser, I.R. Klebanov, A.M. Polyakov, Phys. Lett. B 428 (1998) 105.
[4] J.M. Maldacena, Adv. Theor. Math. Phys. 2 (1998) 231.
[5] J.M. Maldacena, Internat. J. Theoret. Phys. 38 (1999) 1113.
[6] E. Witten, Adv. Theor. Math. Phys. 2 (1998) 253.
[7] E. Witten, Adv. Theor. Math. Phys. 2 (1998) 505.
[8] D. Kubizňák, R.B. Mann, J. High Energy Phys. 2012 (2012) 33.
[9] D. Kastor, S. Ray, J. Traschen, Classical Quantum Gravity 26 (2009) 195011.
[10] M.K. Parikh, Phys. Rev. D 73 (2006) 124021.
[11] M. Cvetič, G.W. Gibbons, D. Kubizňák, C.N. Pope, Phys. Rev. D 84 (2011) 024037.
[12] B.P. Dolan, Classical Quantum Gravity 28 (2011) 125020.
[13] B.P. Dolan, Classical Quantum Gravity 28 (2011) 235017.
[14] B.P. Dolan, Phys. Rev. D 84 (2011) 127503.
[15] W. Ballik, K. Lake, Phys. Rev. D 88 (2013) 104038.
[16] S. Gunasekaran, D. Kubizňák, R.B. Mann, J. High Energy Phys. 2012 (2012) 110.
[17] N. Altamirano, D. Kubizňák, R.B. Mann, Phys. Rev. D 88 (2013) 101502.
[18] N. Altamirano, D. Kubizňák, R.B. Mann, Z. Sherkatghanad, Classical Quantum Gravity 31 (2014) 042001.
[19] S.H. Hendi, M.H. Vahidinia, Phys. Rev. D 88 (2013) 084045.
[20] D. Hansen, Kubizňák, R.B. Mann, J. High Energy Phys. 2017 (2017) 47.
[21] R.G. Cai, L.M. Cao, L. Li, R.Q. Yang, J. High Energy Phys. 1309 (2013) 005.
[22] S. Dutta, A. Jain, R. Soni, J. High Energy Phys. 2013 (2013) 60.
[23] W. Xu, H. Xu, L. Zhao, Eur. Phys. J. C 74 (2014) 2970.
[24] D.C. Zou, S.J. Zhang, B. Wang, Phys. Rev. D 89 (2014) 044002.
[25] H.H. Zhao, L.C. Zhang, M.S. Ma, R. Zhao, Phys. Rev. D 90 (2014) 064018.
[26] N. Altamirano, D. Kubiznak, R.B. Mann, Z. Sherkatghanad, Galaxies 2 (2014) 89.
[27] J.X. Mo, W.B. Liu, Eur. Phys. J. C 74 (2014) 2836.
[28] D.C. Zou, Y. Liu, B. Wang, Phys. Rev. D 90 (2014) 044063.
[29] H. Xu, W. Xu, L. Zhao, Eur. Phys. J. C 74 (2014) 3074.
[30] W. Xu, L. Zhao, Phys. Lett. B 736 (2014) 214.
[31] M.H. Dehghani, S. Kamrani, A. Sheykhi, Phys. Rev. D 90 (2014) 104020.
[32] C.O. Lee, Phys. Lett. B 738 (2014) 294.
[33] J.L. Zhang, R.G. Cai, H. Yu, J. High Energy Phys. 1502 (2015) 143.
[34] M. Zhang, Z.Y. Yang, D.C. Zou, W. Xu, R.H. Yue, Gen. Relativity Gravitation 47 (2015) 14.
[35] J.L. Zhang, R.G. Cai, H. Yu, Phys. Rev. D 91 (2015) 044028.
[36] S.H. Hendi, S. Panahiyan, B. Eslam Panah, M. Faizal, M. Momennia, Phys. Rev. D 94 (2016) 024028.
[37] D. Kubiznak, R.B. Mann, M. Teo, Classical Quantum Gravity 34 (2017) 063001.
[38] X.M. Kuang, O. Miskovic, Phys. Rev. D 95 (2017) 046009.
[39] Y.G. Miao, Y.M. Wu, Adv. High Energy Phys. 2017 (2017) 1095217.
[40] M. Zhang, D.C. Zou, R.H. Yue, Adv. High Energy Phys. 2017 (2017).
[41] S. Weinberg, Phys. Rev. B 138 (1965) 988.
[42] D.G. Boulware, S. Deser, Ann. Physics 89 (1975) 193.
[43] S. Weinberg, Rev. Modern Phys. 61 (1989) 1.
[44] A.G. Riess, et al., (Supernova Search Team), Astron. J 116 (1998) 1009.
[45] Perlmutter, et al., (Surpernova Cosmoly Project), Astrophys. J 517 (1999) 565.
[46] M. Fierz, W. Pauli, Proc. R. Soc. Lond. Ser. A Math. Phys. Eng. Sci. 173 (1939) 211.
[47] H. van Dam, M. Veltman, Nuclear Phys. B 22 (2) (1970) 397.
[48] V. Zakharov, JETP Lett. 12 (1970) 312.
[49] D.G. Boulware, S. Desser, Phys. Lett. B 40 (1972) 227.
[50] D.G. Boulware, S. Deser, Phys. Rev. D 6 (1972) 3368.
[51] R.L. Arnowitt, S. Deser, C.W. Misner, Gen. Relativity Gravitation 40 (2008) 1997.
[52] C. de Rham, G. Gabadadze, Phys. Rev. D 82 (2010) 044020.
[53] C. de Rham, G. Gabadadze, A.J. Tolley, Phys. Rev. Lett. 106 (2011) 231101.
[54] S.F. Hassan, R.A. Rosen, A. SchmidtMay, J. High Energy Phys. 02 (2012) 026.
[55] S.F. Hassan, R.A. Rosen, J. High Energy Phys. 02 (2012) 126.
[56] C. de Rham, Living Rev. Relativ. 17 (2014) 7.
[57] K. Hinterbichler, Rev. Modern Phys. 84 (2012) 671.

[58] T.Q. Do, Phys. Rev. D 93 (2016) 104003.
[59] T.Q. Do, Phys. Rev. D 94 (2016) 044022.
[60] T.Q. Do, J. Phys. Conf. Ser. 865 (2017) 012001.
[61] T.Q. Do, EPJ Web Conf. 206 (2019) 08002.
[62] E. Babichev, A. Fabbri, J High Energy Phys. 2014 (2014) 16.
[63] R.G. Cai, Y.P. Hu, Q.Y. Pan, Y.L. Zhang, Phys. Rev. D 91 (2015) 024032.
[64] H. Kodama, I. Arraut, Prog. Theor. Exp. Phys. 2014 (2014) 023E02.
[65] S.G. Ghosh, L. Tannukij, P. Wongjun, Eur. Phys. J. C 76 (2016) 119.
[66] Y.P. Hu, X.X. Zeng, H.Q. Zhang, Phys. Lett. B 765 (2017) 120.
[67] M. Chabab, et al., Eur. Phys. J. C 79 (2019) 342.
[68] J. Xu, L.M. Cao, Y.P. Hu, Phys. Rev. D 91 (2015) 124033.
[69] B. Mirza, Z. Sherkatghanad, Phys. Rev. D 90 (2014) 084006.
[70] S.H. Hendi, B.E. Panah, S. Panahiyan, J. High Energy Phys. 2015 (2015) 157.
[71] S.H. Hendi, et al., J. High Energy Phys. 2016 (2016) 129.
[72] S.H. Hendi, G.Q. Li, J.X. Mo, S. Panahiyan, B.E. Panah, Eur. Phys. J. C 76 (2016) 571.
[73] S.H. Hendi, R.B. Mann, S. Panahiyan, B.E. Panah, Phys. Rev. D 95 (2017) 021501.
[74] S.H. Hendi, M. Momennia, Thermodynamic description of (a)dS black holes in Born–Infeld massive gravity with a non-abelian hair, arXiv:1801.07906.
[75] D.C. Zou, R.H. Yue, M. Zhang, Eur. Phys. J. C 77 (2017) 256.
[76] M. Zhang, D. Zou, R. Yue, Adv. High Energy Phys. 2017 (2017) 3819246.
[77] X.X. Zeng, H. Zhang, L.F. Li, Phys. Lett. B 756 (2016) 170.
[78] S.H. Hendi, N. Riazi, S. Panahiyan, Ann. Phys. 530 (2018) 1700211.
[79] S.H. Hendi, et al., Phys. Lett. B 781 (2018) 40.
[80] J.-X. Mo, G.-Q. Li, J. High Energy Phys. 2018 (2018) 122.
[81] S.H. Hendi, A. Dehghani, Eur. Phys. J. C 79 (2019) 227.